Adsorptive removal of nickel ions from wastewater by synthesized a novel biocomposite material and process optimization by response surface methodology

Muharrem Ince[a,*], Olcay Kaplan Ince[b], Hevidar Alp[a]

[a]Department of Food Process, Tunceli Vocational School, Munzur University, 62000 Tunceli-Turkey, Tel. +90 428 213 17 94/2404; Fax: +90 428 213 16 24; ORCID ID: 0000-0003-2347-1748, email: muharremince@munzur.edu.tr (M. Ince), ORCID ID: 0000-0001-9167-5844, email: halp@munzur.edu.tr (H. Alp)
[b]Department of Gastronomy and Culinary Arts, Faculty of Fine Arts, Design and Architecture, Munzur University, 62000 Tunceli-Turkey, ORCID ID: 0000-0002-0709-5546, email: olcaykaplan@munzur.edu.tr (O.K. Ince)

ABSTRACT

In the present study, a fixed-bed column study was performed using a novel biocomposite material, *Amanita vaginata* immobilized on Amberlite XAD-4 resin, to find out the adsorption behavior of nickel (Ni^{2+}) ions from industrial wastewater. The influence of some important operating conditions including pH (3–7), biocomposite material amount (150–250 mg (XAD-4:*Amanita vaginata*, 5:1)) influent flow rate (4–8 mL min⁻¹) besides Ni^{2+} ions initial concentration (20–40 mg L⁻¹) on the uptake of Ni^{2+} solution were also optimized using a synthetic water solution. A central composite design combined with response surface methodology was utilized to maximize Ni^{2+} ions removal using *A. vaginata* immobilized on Amberlite XAD-4 resin as a biocomposite material in a column biosorption process. A mathematical model was derived from the central composite design approach for predicting responses and analysis of variance. Also, for checking model adequacy a lack of fit test was carried out. It was determined that the checked and proposed quadratic model was derived from the experimental design data. The biocomposite material adsorption capacity was calculated as 6.28 mg g⁻¹. A high coefficient of determination ($R^2 = 0.9887$) was presented by analysis of variance. Results confirmed that the amount of adsorbed Ni^{2+} amount did not change with the increase of the flow rate ratio and dose when the initial concentration of Ni^{2+} ions increased. The maximum adsorption capacity of biocomposite material was achieved at 6.9 pH, 150.1 mg of biocomposite material amount, 7.8 mL min⁻¹ of solution flow rate, and 39.7 mg L⁻¹ of Ni^{2+} ions initial concentration. Finally, the developed method was applied to industrial wastewater to determine Ni^{2+} ions concentrations.

Keywords: Nickel; Biocomposite material; Adsorption; Fixed-bed column; Regression model

1. Introduction

Recently, heavy metal pollution has become a chronic problem for the ecosystem because of the threat to all living things, especially, human health. They enter human life via global industrialization and man-made industrial activities. Heavy metals especially Hg, As, Ni, Cu, and Cr, or their compounds are now recognized as dangerous pollutants. Because they are non-biodegradability have a constant presence in the food chain and have the potential to accumulate easily in living organisms due to their lipophilic properties, also. Therefore, monitoring foods contaminated by heavy metals is a vital issue for humans [1]. Among these hazardous metals' Ni was preferred for removal from aqueous media. Because Ni compounds have

* Corresponding author.

widespread applications in various industrial processes such as paint formulation, battery manufacturing, and mineral processing [2].

Nickel compounds have a carcinogenic effect and are easily absorbed when they contact the skin [3]. In the case of prolonged or high dose exposure to Ni compounds, they cause health problems including asthma, gastrointestinal distress, lung cancer, lung embolism, allergic reactions, skin rashes, heart disorders, and even Ni^{2+} ions are toxic at low concentrations [2,4,5]. In addition, when Ni was accumulated in the human body can lead to several diseases and disorders mainly cardiovascular and kidney disease along with malignant tumors [6,7].

Various health organizations have restricted the Ni^{2+} ions concentration due to its serious toxic and carcinogenic effects. For example, while the US EPA has set specific Ni^{2+} ions limits as 0.2 mg L^{-1} for long-term effluent reuse, the maximum acceptable concentration of Ni^{2+} ions in drinking water was limited to 0.02 mg L^{-1} by the World Health Organization (WHO) [8–10]. Also, in drinking water, permissible Ni^{2+} ions limits were reported as 0.01 mg L^{-1} by WHO [11].

Several technologies are available to remove heavy metals from an aqueous medium. Some of these methods are ion-exchange/solvent extraction, reverse osmosis, biological operations, chemical precipitation, ultrafiltration, and adsorption [12,13]. Because of sludge production, the precipitation method has a major disadvantage. Although ion exchange is considered a better alternative technique, it suffers from its high operating cost. In other words, it is out of choice in this technique due to the high operating cost [14]. Among the available techniques, the adsorption method has a wide range of uses due to its simplicity of application, efficiency, and low-cost advantage [10]. In addition to the ability of biological materials to biosorbate metal ions, they have a wide range of uses for the development of new technologies in this field. Biological materials are cheap and clean for wastewater treatment [15]. For evaluating sorbents' sorption capacity in an aqueous medium, batch experiments are generally used to obtain sorption isotherms equilibrium [16]. On the other hand, fixed-bed columns are preferred for full-scale biosorption processes, also. It is important to remember that without a quantitative approach, a priori design and optimization of fixed-bed columns are difficult [17].

Over the last few years, there have been numerous studies about metals removal using various materials by batch adsorption technique. On the other hand, there is only limited research about the preparation of fungus using *A. vaginata* and its application to the removal of Ni^{2+} ions from various industrial wastewaters (IW). Recently, researchers have focused on utilizing new chelating materials for metal ion enrichment because chelating materials have been functionalized in several support materials such as XAD-4 and XAD-7, which are commercially available polymeric resins. It has been preferred in much research because of several superior chemical properties such as durability, high surface area, porosity, and purity for pre-concentration procedures. Also, for preparing a ligand-loaded resin, XAD-4 has been widely used as a solid sorbent. The mentioned resin, interacting with various ligands as complexing materials, was used for heavy metal pre-concentration [18–20]. There are very limited studies on chelating agents by immobilizing biological materials like *A. vaginata* on resins such as XAD-4 [19,21,22]. Fixed-bed columns system have been preferable to batch experimental design, in practical industries, to remove metals as continuous flow [23]. When the metal solution interacts with a fixed-bed column, metal ions load onto the adsorbents and flow continues through the packed bed. Fixed-bed column sorption systems that are proper design, especially in the application of industrial scale, are vital for providing basic data [24]. In a continuous fixed-bed column system, biosorption with immobilized biomass is typically performed [25], because of its mechanical strength besides proper size, which is imperative for large-scale treatment of IW [26].

To evaluate *A. vaginata* immobilized on Amberlite XAD-4 resin Ni^{2+} ions removal efficiency, column process variables need to be optimized. Conventional techniques are not in demand due to the need for many experimental studies. Instead of conventional techniques, a statistical experimental design approach preference is more advantageous. The major disadvantage of these methods can be expressed as the inability to determine the interaction between the process variables on the dependent variable. To overcome such a problem is possible only by reducing the number of experiments, but also by using a statistical experimental design that provides a suitable model for process optimization that allows the evaluation of effects between variables. Recently, various experimental design methods, including response surface methodology (RSM), are frequently used for multivariate physicochemical process optimization [27,28]. The RSM is a useful statistical tool that is preferred and frequently used for understanding the effect of many variables affecting the responses by doing limited experiments. It was of great importance to use a new adsorbent as a fixed-bed column, since there are a limited number of studies examining the effects of parameters affecting the removal and adsorption of Ni^{2+} ions using biocomposite materials.

In this study, *A. vaginata* which is biological material was preferred and it was immobilized on Amberlite XAD-4 resin. Obtained biocomposite material was carried out for the removal of Ni^{2+} ions from various IW. Due to their cell wall structure, fungi belonging to the Basidiomycetes class are frequently preferred in biotechnological studies. Because the polysaccharides found in the cell wall of the white-rot fungus, especially the chitin layer, have a high binding capacity for metals [29,30]. It is known that the lactase enzyme, which is extracellular synthesis by these fungi, plays an active role in various dangerous metals removal from an aqueous medium. This study investigates the ability of biocomposite material-removing Ni^{2+} ions from an aqueous medium using a fixed-bed column system. The present study's aims can be summarized as follows: (1) Using a central composite design (CCD) optimization methodology to obtain biocomposite material maximum adsorption capacity; (2) to investigate four independent variable's effect on Ni^{2+} ions adsorption and their interactions for Ni^{2+} ions removal; (3) to verify proposed model validity by using analysis of variance (ANOVA); (4) to optimize column conditions; and (5) to apply the developed method to real samples (IW) for determination of Ni^{2+} ions levels.

2. Materials and methods

2.1. Chemicals and instruments

The XAD-4 resin, Ni²⁺ ions standard solution, NaOH, and HCl were purchased from Alfa Aesar Company (Karlsruhe, Germany) and Merck Company (Darmstadt, Germany). All used chemicals were of the highest commercially available, typically 99.9% or higher, and analytical reagent grade. The *A. vaginata* immobilized XAD-4 resin and Ni²⁺ loaded *A. vaginata* immobilized XAD-4 resin was performed using Fourier-transform infrared spectroscopy (FTIR)-ATR spectrophotometer (ATR: attenuated total reflectance; 67000, Japan). Biocomposite material and Ni²⁺ ions loaded surface morphology of biocomposite material and X-ray analysis were made using a digital scanning electron microscopy-energy-dispersive X-ray spectrometer (Hitachi SU3500, Japan) and X-ray diffractometer (Rigaku MiniFlex-600, Japan), respectively. To optimize the flow rate in the column system a Shenzhen peristaltic pump (Wertheim, Germany) was used. An ultrapure water system (ELGA LabWater/VWS, UK) was used throughout the experiment. A bench top pH meter (EZDO; PL-700PV) was used for pH measurements.

2.2. Preparation of fungal biomaterial and XAD-4 resin

A. vaginata, collected from Tunceli, Turkey, was used as the biomaterial in the present study. Before being used, it was cleaned using tap water and then ultrapure water for removing contaminants. The cleaned biomaterial was dried using the air-dried oven for 72 h at 45°C. Air-dried fungal biomaterial was ground in a porcelain mortar for obtaining proper powder. The powder was then dried in an oven at 80°C for 24 h to achieve the complete death of all cells. Ultimately, the cells were inoculated into a malt agar at 25°C for 24 h. The absence of mycelia of *A. vaginata* showed positive results, indicating the complete death of the fungus. Amberlite XAD-4 resin (non-ionic polystyrene adsorbent, approximate surface area 750 m² g⁻¹) was supplied by Alfa Aesar Company (Karlsruhe, Germany) and used as support material. Organic and inorganic impurities and contaminants contained in the resin were removed with 1 M NaOH, 4 M HCl, and C₂H₅OH. It was firstly rinsed with 1 M NaOH (2 h) and washed with ultrapure water until its pH was neutral, then with 4 M HCl (2 h), and finally with C₂H₅OH and ultrapure water again. Prior to contact with fungus (*A. vaginata*), cleaned Amberlite XAD-4 was dried at 60°C (12 h) in the oven.

2.3. A. vaginata immobilization on Amberlite XAD-4

To obtain a biocomposite material, the immobilization of biomaterial (*A. vaginata*) onto the polymeric resin was carried out as follows: fungus powder of about 500 mg was mixed with 5 g of polymeric resin. The mixture was wetted with about 3 mL of ultrapure water several times. For maximizing the contact between resin and biomass, the wetting and drying steps were repeated at least five times. Thus, thorough mixing was achieved the immobilization efficiency was increased. Moreover, for improving the efficiency of immobilization, the mixture was heated in an oven at 60°C for 24 h to obtain dry biocomposite material.

The dried mixture was milled to a size of less than 120 mesh and used as an adsorbent for Ni²⁺ ions removal from various IW. Turbidity analysis was performed to determine whether the fungal-resin interaction was successful and immobilization efficiency. These analyses revealed that all fungus mass (500 mg) was immobilized on polymeric resin.

2.4. Preparation of the column and adsorption–desorption studies

Specified amount (range from 100 to 300 mg) by the CCD (Table 1), biocomposite material was transferred to a 0.5 cm × 10.0 cm solid-phase extraction polyethylene column. Before using, approximately 10 mL of ultrapure water was passed through the column for column conditioning and cleaning. The influence of important operating conditions, including pH (3–7), solution flow rate (4–8 mL min⁻¹), and initial Ni²⁺ ions concentration (20–40 mg L⁻¹), on the uptake of Ni²⁺ ions solution, were identified by using CCD. The model solution was passed through the prepared column by using a peristaltic pump to adjust the flow rate. Then the retained Ni²⁺ ions on the fungal biomaterial were eluted using the procedure that is explained in the sample preparation step. The Ni²⁺ ions concentration in this solution was determined by using a flame atomic absorption spectrometer (Flame-AAS).

2.5. Preparation of industrial wastewater for analysis

Acidified IW with concentrated HNO₃ (for 50 mL of sample, 3 mL of concentrated HNO₃ was used) was degassed, by using an ultrasonic water bath at 40°C for about 30 min [31]. After the acidification and degassing process, to prevent contamination, samples were placed into 250 mL glass beakers and covered with watch glasses in order. Then, each sample was treated using the optimized method and made ready to be transferred to the column. All samples were passed the column. Then, the biocomposite material, that was used as column filling material, was treated with 3 mL of 0.2 M HNO₃. Analytical blanks were prepared in a similar manner and clear solutions were subsequently analyzed by using flame-AAS. All samples were prepared in triplicate and Ni²⁺ ions concentrations were determined.

2.6. Analytical method

An experiment process was performed to achieve Ni²⁺ ions concentration from an aqueous solution. A calibration curve was created for calculating adsorbed Ni²⁺ ions before the real samples' concentrations were determined. For this purpose, using Ni²⁺ ions standard solutions with known concentrations (from 0.1 to 2 mg L⁻¹) process was performed. The amount of adsorbent determined by experimental design (Table 1) was filled the column and 50 mL of Ni²⁺ solutions of initial concentrations (20–40 mg L⁻¹) pH (range from 3–7) was adjusted with (0.01–0.1 N) HCl and (0.01–0.1 N) NaOH. Using a peristaltic pump, prepared solutions were passed from the column. To elution of Ni²⁺ ions from the surface of biocomposite material, 0.5 M HCl solution was used for the desorption process. Ni²⁺ ions concentration of elution was measured to understand whether it contains Ni²⁺ ions by using flame-AAS. By using the

Table 1
Experimental factors and levels in the CCD

Factors	Levels			Star point α = 2	
	Low (–1)	Central (0)	High (+1)	–α	+α
(X_1) pH	3	5	7	1	9
(X_2) Biocomposite material amount (mg)	150	200	250	100	300
(X_3) Flow rate (mL min^{-1})	4	6	8	2	10
(X_4) Initial concentration (mg L^{-1})	20	30	40	10	50

Run	X_1	X_2	X_3	X_4	Experimental values (mg g^{-1})	Predicted values (mg g^{-1})
1	1	200	6	30	0.88	1.00
2	3	250	4	40	1.97	2.01
3	7	150	4	20	0.76	0.80
4	5	200	6	30	1.75	1.67
5	3	250	8	40	0.98	1.09
6	3	250	8	20	1.98	2.09
7	5	200	2	30	0.63	0.67
8	3	150	4	20	1.49	1.54
9	5	200	6	30	1.42	1.42
10	7	150	8	20	2.40	2.43
11	9	200	6	30	1.18	1.22
12	7	250	8	40	1.99	2.09
13	3	150	8	40	1.53	1.51
14	7	150	4	40	2.51	2.51
15	3	250	4	20	1.12	1.09
16	5	200	6	30	1.95	1.96
17	5	200	6	10	0.32	0.24
18	3	150	8	20	2.17	2.11
19	7	250	4	40	2.37	2.25
20	7	150	8	40	1.50	1.49
21	5	200	6	30	1.70	1.64
22	5	200	6	30	1.67	1.60
23	7	250	4	20	1.27	1.20
24	5	100	6	30	1.95	2.04
25	5	200	6	50	1.59	1.62
26	3	150	4	40	1.68	1.62
27	5	300	6	30	1.63	1.62
28	5	200	10	30	1.57	1.62
29	5	200	6	30	1.66	1.62
30	7	250	8	20	1.73	1.62

Constant parameters: temperature, room temperature; solution volume, 20 mL; mixing speed, 150 rpm

following equation, adsorbed Ni^{2+} ions amount by the unit mass of adsorbent was calculated.

$$q = \frac{(C_0 - C_e)V}{m} \tag{1}$$

where q (mg g^{-1}), C_e and C_0 represent the amount adsorbed per gram of adsorbent, equilibrium concentrations, and Ni^{2+} ions solution initial concentration (mg L^{-1}),

respectively. Accordingly, the used adsorbent mass represents by m and V (L) refers to the initial concentration of Ni^{2+} ions solution.

To determine the reusability of biocomposite adsorbent some experiments were performed. The Ni^{2+} ions solution (40 mg L^{-1}, 20 mL) under optimum conditions determined by the CCD approach was treated with biocomposite material. These application studies were repeated at least 8 times.

2.7. Matrix effects

In an adsorption process, matrix ions can affect the recovery or removal values since they can compete with the analyte for the binding sites. Based on this reason, the matrix ions effect in natural samples is one of the most important problems for trace elements detection with instrumental techniques, that is, matrix effects. For this purpose, the matrix ions effect was also examined. The optimized and developed method was carried out for modeling solutions containing matrix ions and Ni^{2+} ions under optimum conditions. In order to determine the matrix ions effect, it was applied by making minor changes in the study of Özkantar et al. (2020). Matrix ions tolerance limit could be defined as the ion concentrations affecting the analyte ions lower than 5%. Obtained results prove that developed and proposed biocomposite material supported installed on the fixed-bed column and optimized with the CCD method can be successfully applied even in the presence of matrix ions. In this study, some inorganic species' tolerable levels are suitable for Ni^{2+} ions pre-concentration and separation from real samples including IW.

2.8. Experimental design and optimization

The RSM which is a collection of mathematical and statistical techniques is beneficial for analyzing the effects of several independent variables on the response. The RSM approach, known as regression analysis, is used to establish relationships between variables, estimate parameters, and obtain data as well as correlate test indexes with continuous variables [32]. First of all, CCD makes it easy to design experiments statistically and to estimate the coefficients in a mathematical model. Ultimately, it is accepted as a convenient option for predicting the answer and checking the adequacy of the model. Recently, the use of the design of experiments has boomed. It is preferred in the design of many studies as it has a wide range of applications including in the food industry, chemicals, and pharmaceuticals [33,34].

In the present study, four factors with five levels were preferred for studying and optimizing the process variable's influence. The specified parameters have been preferred because they have a significant effect on adsorption. Also, an experimental design program, CCD, was used to optimize process variables and their interactions. Also, the optimization procedure ensures some advantages including model adequacy checking and predicting of response besides coefficients estimation of mathematical model [35]. Both to examine the response of all variables' maximum area and identify the optimum value region this method was used. Used all factors coded as "−α," "−1", "0", "+1", and "+α". A CCD combined with RSM was utilized for determining maximum Ni^{2+} ions adsorption by biocomposite material filled into a column. Based on preliminary experiment studies, four critical variables affecting Ni^{2+} ions adsorption were chosen as independent variables, and adsorption of Ni^{2+} ions on biocomposite material (Y) was considered as the dependent variable. An equation that is second-order polynomial was derived from the regression analysis and presented in Eq. (2):

$$Y\left(\frac{\text{mg Ni/g biocomposite}}{\text{material}}\right) = -0.73 + 0.64X_1 - 6.73X_2$$
$$+ 0.09X_3 + 0.04X_4 - 3.45X_1X_2 - 3.26X_1X_3$$
$$- 1.05E - 0.03X_1X_4 - 5.19E - 0.04X_2X_3$$
$$- 5.53X_2X_4 + 1.14E - 0.03X_3X_4 - 0.02X_1^2$$
$$+ 2.36X_2^2 - 1.01X_3^2 - 2.24E - 0.04X_4^2 \qquad (2)$$

Three operations including 2k, axial runs, 2^k, factorial runs, and central runs have been used to characterize CCD. For CCD characterization, these operations are generally used including axial runs (2k), factorial runs (2^k), and central runs. The present study has 8 axial points, 16 factorial points, and 6 center points. A total of 30 experiments were designed by CCD (Table 1).

$$N = 2k + 2^k + n_c \qquad (3)$$

where k and n_c represent the factors number and the center points number, respectively. Distance between the center point and the axial point is represented by the alpha (α) term and it depends on the rotational number and factorial points. Furthermore, α can be calculated by using Eq. (4) [36,37]:

$$\alpha = 2^{(k/4)} \qquad (4)$$

Experimental results obtained from optimization studies were confirmed by using experiments that are identified by the quadratic model. The model predicted values which confirm by CCD efficiency were undoubtedly similar to corresponding experiment results. For optimizing the experimental variables based on data obtained from the design methodology, the CCD is the perfect approach. Because in the process of removing Ni^{2+} ions, very important results have been obtained using biocomposite materials. The predicted model values, confirming the effectiveness of the used model, were observed to be significantly similar to the corresponding experiments. It is clear that the best method is to use the surface plot, and with these plots, it is possible to determine the optimum point and achieve the highest purification performance. It is good evidence that the difference between the predicted and experimental results can be ignored in both proposed quadratic models' efficiency and in predicting the optimum conditions. Table 1 presents Ni^{2+} ions adsorption amount, independent variables, and their levels' experimental range. A design program (Design-Expert Version 10, Stat-Ease, USA) was utilized for proposing a regression model that was derived by analyzing the experimental results. Various parameters including variable conditions, predicted, and experimental values were given in Table 2. Also, diagnostic checking tests provided by ANOVA were performed for adequacy model check. The convenient polynomial model is characterized using the determination coefficient of R^2. Also, determination coefficient values provide a measure of how variability can be clarified thanks to experimental factors and their interactions. Furthermore, the 'F'-test and p-value of Fisher's were analyzed [38].

Table 2
Analysis of variance (ANOVA) for the quadratic polynomial model

Source	Sum of squares	df	Mean square	F-value	p-value Prob. > F	
Model	7.80	14	0.56	93.85	<0.0001	Significant
X_1-pH	5.27	1	5.27	887.76	<0.0001	
X_2-Biocomposite material amount	0.86	1	0.86	144.38	<0.0001	
X_3-Flow rate	2.485E-003	1	2.485E-003	0.42	0.5273	
X_4-Initial concentration	1.05	1	1.05	177.11	<0.0001	
X_1X_2	0.019	1	0.019	3.21	0.0933	
X_1X_3	2.714E-003	1	2.714E-003	0.46	0.5091	
X_1X_4	7.062E-003	1	7.062E-003	1.19	0.2925	
X_2X_3	0.043	1	0.043	7.27	0.0166	
X_2X_4	0.012	1	0.012	2.06	0.1713	
X_3X_4	8.292E-003	1	8.292E-003	1.40	0.2556	
X_1^2	0.36	1	0.36	60.55	<0.0001	
X_2^2	0.096	1	0.096	16.16	0.0011	
X_3^2	4.498E-004	1	4.498E-004	0.076	0.7868	
X_4^2	0.014	1	0.014	2.31	0.1491	
Residual	0.089	15	5.9E-003			
Lack of fit	0.073	10	7.3E-003	2.20	0.1989	Not significant
Pure error	0.016	5	3.3E-003			
Cor. total	7.89	29				
R-squared	0.9887					
Adj. R-squared	0.9782					
Pred. R-squared	0.9440					
Adeq. precision	41.719					

$p < 0.01$ highly significant; $0.01 < p < 0.05$ significant; $p > 0.05$ not significant
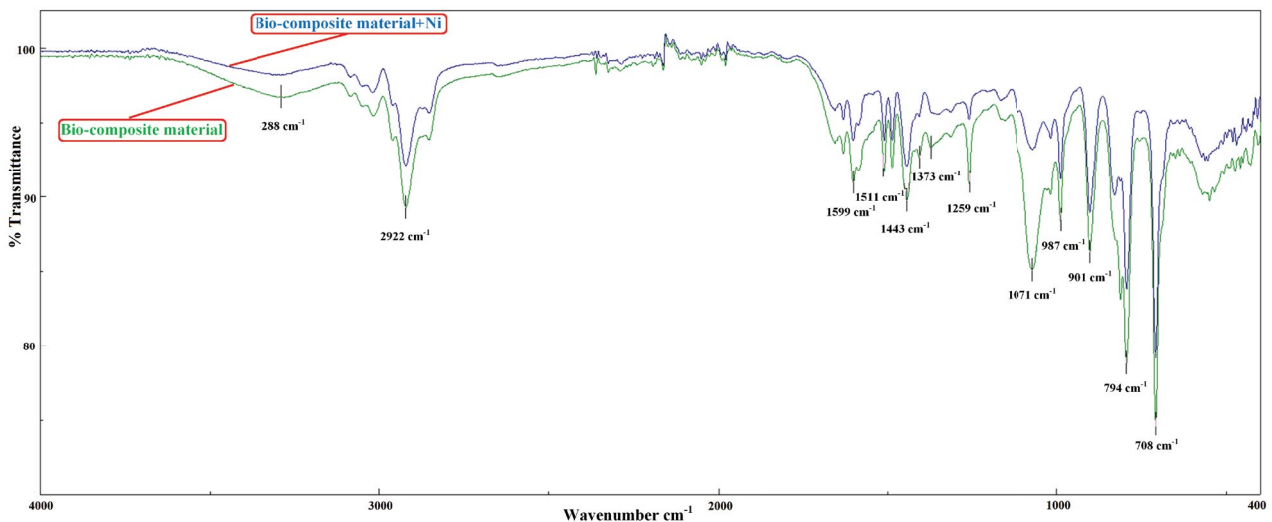

Fig. 1. FTIR spectra of biocomposite material and Ni^{2+}-loaded biocomposite material.

3. Results and discussion

3.1. Characterization of adsorbent

3.1.1. Fourier-transform infrared spectroscopy

Spectra of the pre-treated biocomposite material and Ni^{2+} ions loaded biocomposite material were compared (Fig. 1) by using FTIR. The recorded spectra frequency range was 4,000–500 cm^{-1}. The shifts and changes in the FTIR bands during Ni^{2+} ions loaded on the *A. vaginata* immobilized on Amberlite XAD-4 resin are shown in Fig. 1. Major changes were observed in 3,288; 2,922; 1,599; 11,259 and 1,071 cm^{-1}. The changes and shifts that occurred can be summarized as follows: FTIR spectra of Ni^{2+} ions loaded

A. vaginata immobilized on Amberlite XAD-4 resin showed a band around 3,288 cm^{-1} because of the presence of OH group and at 2,922 cm^{-1} weak asymmetric stretching of C–H. While the observed band is around 1,599 cm^{-1} strong symmetric and the asymmetric stretching of C=O, the band at 1,373 cm^{-1}, is due to C–(CH$_3$)$_2$ bending. The band for the Ni^{2+} ions-loaded biocomposite material can be assigned as 1,071 cm^{-1} (skeletal vibration of C–O). The biocomposite material showed lower intensity peaks at 3,288; 2,922; 11,599; 1,259 and 1,071 cm^{-1} compared with the Ni^{2+} ions loaded biocomposite material, suggesting a disruption of some of these groups during treatment.

3.1.2. Second-order polynomial model

Tables 1 and 2 illustrate ANOVA test results. It contains suggested second-order equation coefficients and model terms for Ni^{2+} ions adsorption on biocomposite material. Fisher test was chosen because it shows that the smaller *p*-values and larger *F*-values point out more meaningful the proposed model terms.

If the *p*-values of ANOVA are less than 0.05, it is indicated a significant regression in the 95% confidence level. It can be stated that based on ANOVA, the *F*-value of this study is 93.85, indicating that the model is important. On the other hand, significant model terms are determined by their "Prob. > *F*" values. When these values are less than 0.05 indicate model terms are significant statistically. According to "Prob. > *F*" values; as X_1, X_2, X_4, X_1^2, and X_2^2 are highly significant, X_1X_2, X_3X_4 are significant model terms. Conversely, X_3, X_1X_3, X_1X_4, X_2X_4, X_3X_4, X_3^2, and X_4^2 model terms are not significant values, since their values are greater than 0.5. Lack of fit (LOF) *p*-values measures the fitness of the model and these values imply the LOF is not significant in relating to the pure error. The present study's LOF *F*-value is 0.97 and it expresses the LOF is not significant relative to the pure error. The goodness of fit model was evaluated by using R^2 and R^2_{adj} values. Also, it is desired that the R^2 value be greater than at least 0.75. Because this value defines the percentage of variability in the response, it is desirable that the R^2 values of the proposed model be high, moreover close to 1 value. The model R^2 and R^2_{adj} values previously mentioned were satisfactory. Because the R^2 was obtained as 0.9887, it can be said that 98.87% of the model-predicted values matched the experimental adsorbed Ni^{2+} ions values on biocomposite material. There is a good concordance between predicted (R_{predic}) and experimental (R_{exp}) responses according to the residual analysis outlines. The quadratic model adequacy was investigated by using residuals ($e = R_{exp} - R_{predic}$) assessment. Additionally, the difference between the "R^2_{predic}; 0.9440" and "R^2_{adj}; 0.9782" is less than 0.2, it is possible to say that these values are largely compatible. Model signal to noise ratio is measured by the "Adeq. Precision" value and this ratio greater than 4 is desirable. Moreover, signal to noise ratio of the present study is 130.6 and it indicates an adequate signal. Based on statistical results obtained from ANOVA, it can be stated that predicting levels of Ni^{2+} ions using a statistical model was adequate.

3.1.3. Response surface methodology analysis

Based on experimental results, for the determination of response points as maximum, minimum, and middle three-dimensional (3D) response surface graphs were created using a quadratic model. Because these graphs are useful. Figs. 2 and 3 represent each parameter's effects on Ni^{2+} ions removal from wastewater, and the interaction of these parameters. Also, the impact of pH-adsorbent
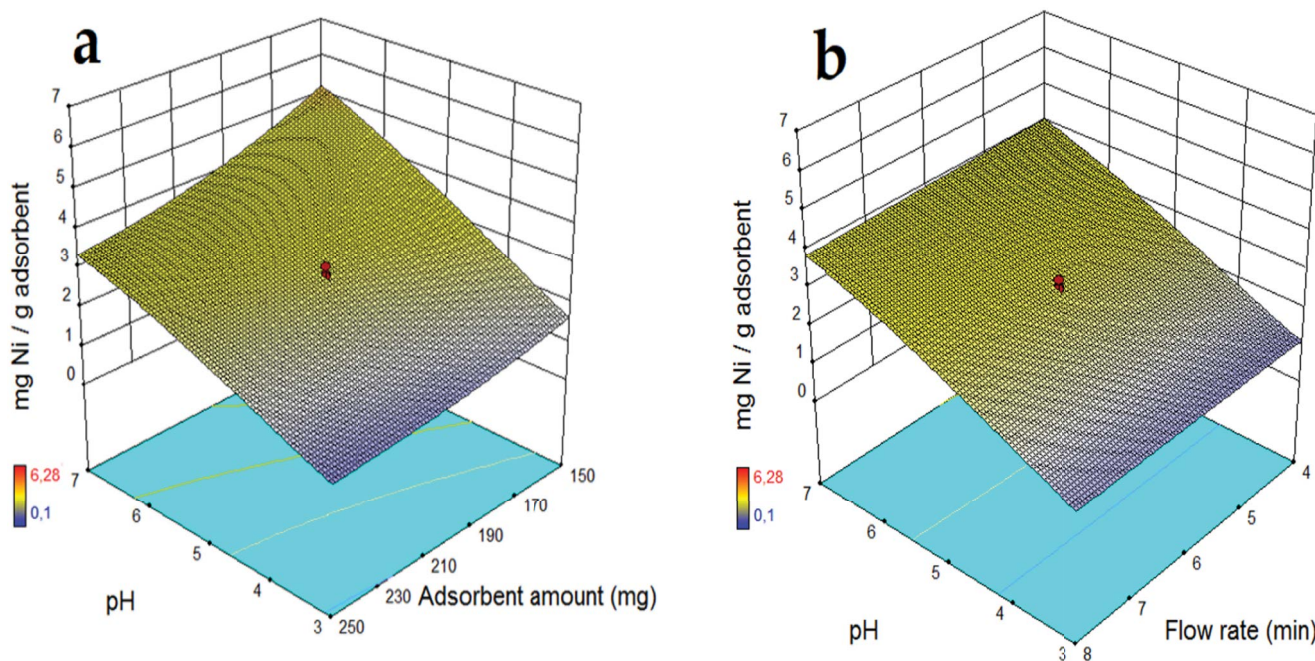

Fig. 2. 3D response surface graphs for Ni^{2+} adsorption on biocomposite material for the interactive effect of (a) pH-adsorbent amount and (b) pH-flow rate.

amount, pH-flow rate, Ni^{2+} ions initial concentration-pH, and adsorbent amount-Ni^{2+} initial concentration on Ni^{2+} ions removal using biocomposite material was illustrated. It is clear that the removal of Ni^{2+} ions amount increased with the increase of pH up to 7 and decreased biocomposite material amount the removal of Ni^{2+} ions efficiency (Fig. 2a). Fig. 2b shows that Ni^{2+} ions removal from the aqueous medium was strongly influenced by the pH. Fig. 3c illustrates a 3D response surface graph of the influence of Ni^{2+} ion's initial concentration-pH on the adsorption efficiency of Ni^{2+} ions biocomposite material. While, it is clear that the Ni^{2+} ions adsorption increased with decrease of adsorbent amount ($p < 0.01$) up to 150 mg, Ni^{2+} ions initial concentration change (from 20 to 40 mg L^{-1}) show a significant effect on Ni^{2+} ions adsorption ($p < 0.01$) (Fig. 3d). Based on the ANOVA table and 3D graphs, pH and Ni^{2+} ion's initial concentration are significantly efficient process parameters ($p < 0.0001$). As can be seen clearly, with an increase

in the pH up to 7 and decreases in adsorbent amount, Ni^{2+} removal increases from aqueous media.

Additionally, experiment numbers were sufficient for determining the effects of the independent variables for Ni^{2+} ions removal from aqueous solutions using biocomposite material. Obtained results revealed that using a statistical model was adequate for predicting Ni^{2+} ions levels and actual, predict, and residual values profiles of experimental design are shown in Fig. 4.

To compare the effect of all studied factors on optimum conditions for Ni^{2+} ions removal a perturbation plot was carried out (Fig. 5). In addition, it was utilized for the combined effect of all the factors on a process besides for analyzing the variation of the factors. It has been observed that almost all factors, especially Ni^{2+} ion's initial concentration and pH, are seriously effective in Ni^{2+} ions removal. In addition, for the check of the lambda (λ) value Box–Cox plot was used. To enhance the model significance, it is often preferred for
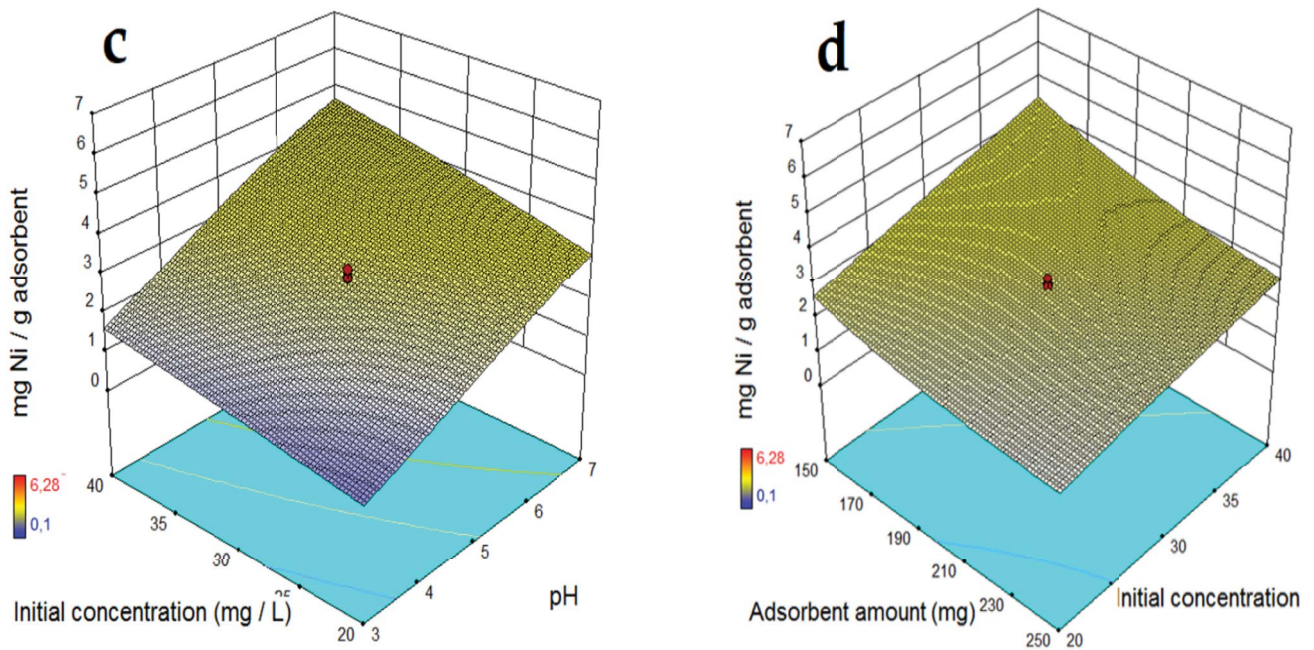

Fig. 3. 3D response surface graphs for Ni^{2+} adsorption on biocomposite material for interactive effect of (c) initial concentration-pH and (d) adsorbent amount-initial concentration.

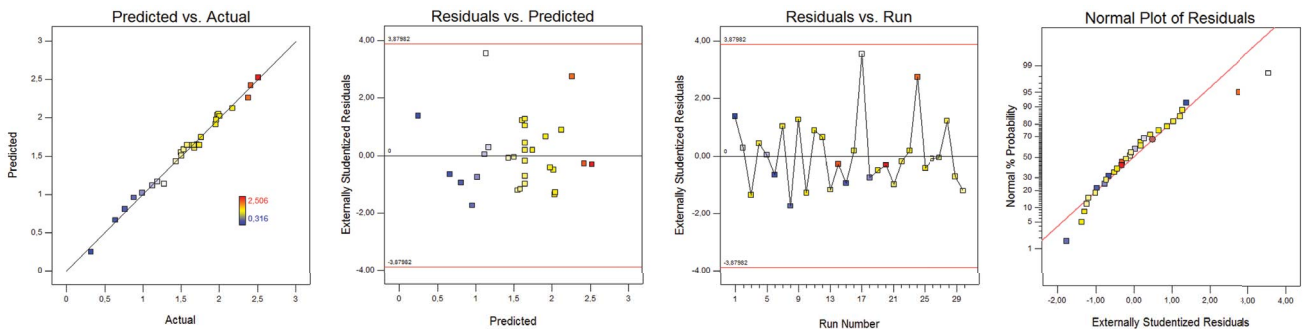Fig. 4. Diagnostic plots for Ni^{2+} optimization process using CCD. (a) Actual and predicted, (b) normality, (c) studentized residuals and predicted, and (d) studentized residuals and run values of Ni^{2+}.

predicting any necessary transformation of the experimental value. Based on the 0.50 λ-value obtained from the Box–Cox plots, a power transformation (square root) was used. The optimum values of the variables used for optimization and the highest desirability values besides the ramp chart for statistically optimize factors for Ni^{2+} ions removal obtained depending on these values are presented in Figs. 6 and 7.

3.1.4. Nickel ions removal performance of biocomposite material

Based on the possible global solution (Table 3), for supporting the optimized data obtained from numerical modeling under optimum conditions (pH of 6.9, biocomposite material amount of 150.1 mg, solution flow rate of 7.8 mL min^{-1}, initial Ni^{2+} concentration of 39.9 mg L^{-1}) the confirmatory experiments were performed. The obtained experimental results were also compared with the probable Ni^{2+} ions removal results suggested by the quadratic model and it was observed that the confirmation values matched with the proposed model results as 99.8%. The optimum conditions IW were analyzed and Ni^{2+} ions concentrations of samples are given in Table 4. Some of the wastewater samples examined in terms of Ni^{2+} ions content consists of the wastewaters of the industrial region where metal operations are carried out intensively. Another part was taken
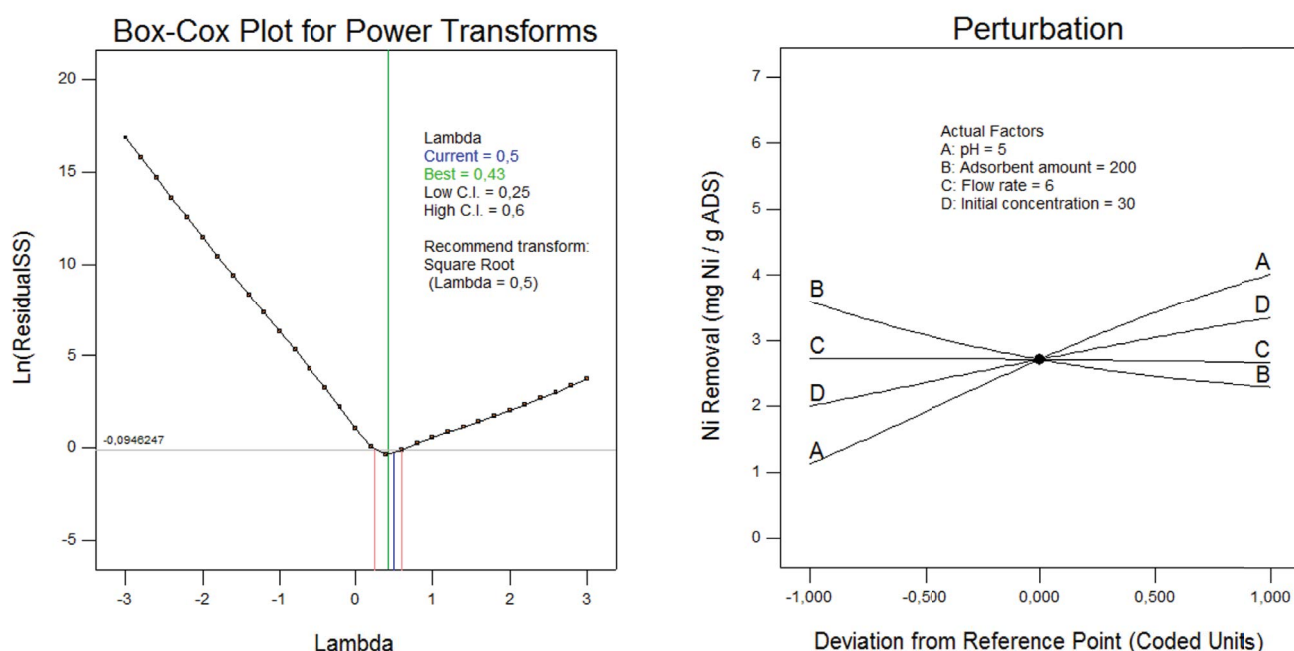

Fig. 5. Diagnostic plots: Box–Cox plot and perturbation plot for Cd removal at the optimal conditions: solution pH 6.995 (A), adsorbent amount 150.071 mg (B), solution flow rate of 7.836 mg L^{-1} (C), and Ni^{2+} initial concentration 39.934 mg L^{-1} (D).
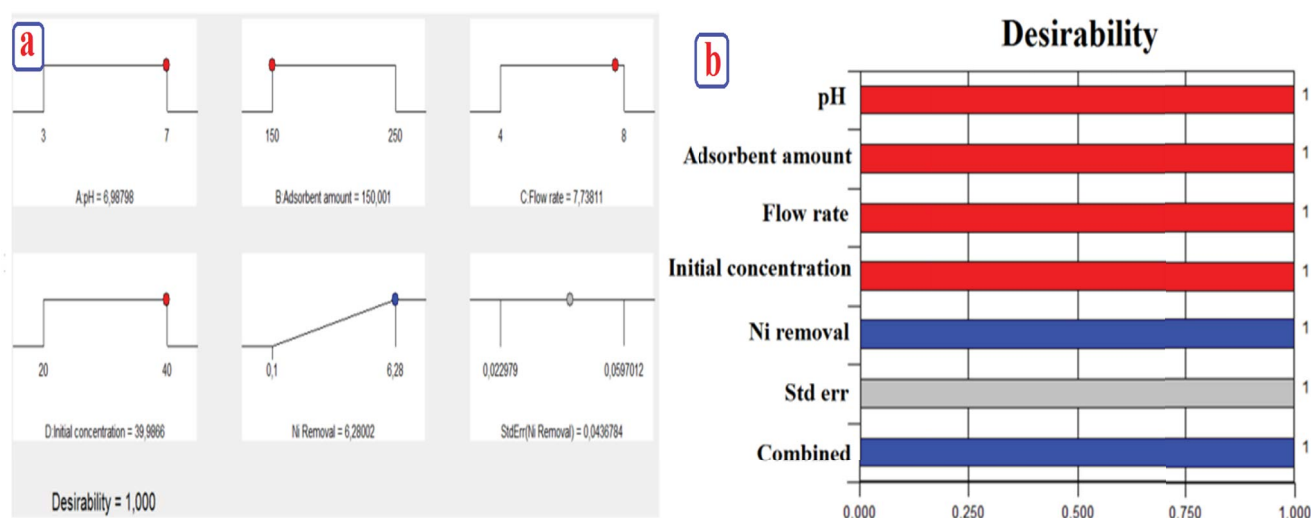

Fig. 6. (a) Ramp chart and (b) desirability for statistically optimized factors for Ni removal.

from the area where the ferrochrome factory wastewater was discharged. In industrial zones, regions, where leather, dye and similar businesses are concentrated were preferred.

Although many studies have been carried out recently for the removal of Ni^{2+} ions, there are several reasons why this study is different from its counterparts. These advantages can be summarized as follows: (1) It can be stated that this biocomposite material shows extraordinary performance for Ni^{2+} ions removal. (2) It can be mentioned that, based on column studies, this hybrid material could be utilized as an efficient adsorbent for the clean-up of the environmental, also. The adsorption capacity of the used material in this study was calculated as 6.28 mg g^{-1}. Table 5 presents
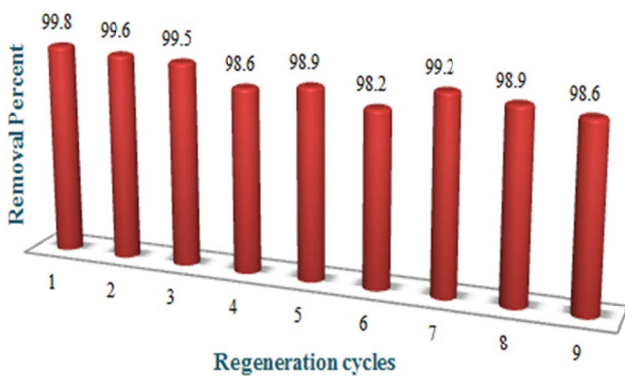
the maximum sorption capacity of the various adsorbent types used for the removal of Ni^{2+} ions. The biocomposite material used in this study's adsorption capacity is higher than several adsorbents in most of the previous studies for Ni^{2+} ions removal. So, this biocomposite material has some

Fig. 7. Biocomposite material reuse performance.

Table 4
Removal of Ni^{2+} ions using biocomposite material from IW

Sample	Ni^{2+} (μg L^{-1})		
	SA	Found (SD)	Removal (%)
	0.0	88 ± 5	
IW-1	40	125 ± 7	98
	80	170 ± 12	100
	0.0	58 ± 4	
IW-2	40	98 ± 6	100
	80	136 ± 8	99
IW-3	–	46 ± 3	
IW-4	–	72 ± 12	
IW-5	–	89 ± 12	
IW-6	–	52 ± 5	
IW-7	–	68 ± 4	
IW-8	–	47 ± 3	
IW-9	–	62 ± 4	
IW-10	–	47 ± 2	

SA: Standard addition; SD: Standard deviation

Table 3
Possible global solutions for maximum Ni^{2+} ions removal from IW

				Solutions				
Number	pH	Adsorbent amount	Flow rate	Initial concentration	Ni removal	StdErr(Sqrt(Ni removal))	Desirability	
1	6.9	150.0	7.7	39.9	6.280	0.044	1.000	Selected
2	6.9	150.3	7.9	39.8	6.284	0.045	1.000	
3	7.0	150.0	8.0	40.0	6.317	0.046	1.000	
4	7.0	150.2	7.8	39.9	6.281	0.044	1.000	
5	6.9	150.1	7.8	39.9	6.283	0.045	1.000	
6	7.0	150.7	7.9	40.0	6.279	0.045	1.000	
7	6.9	150.1	8.0	39.9	6.266	0.045	0.998	
8	7.0	150.0	7.5	39.9	6.265	0.042	0.998	
9	6.9	150.2	8.0	40.0	6.238	0.045	0.993	
10	7.0	150.0	7.2	40.0	6.237	0.041	0.993	
11	7.0	150.0	7.1	40.0	6.225	0.040	0.991	
12	7.0	150.0	7.4	39.5	6.217	0.042	0.990	
13	6.9	150.1	8.0	39.0	6.209	0.045	0.988	
14	7.0	150.0	6.8	39.9	6.201	0.039	0.987	
15	7.0	152.0	8.0	39.6	6.201	0.044	0.987	
16	7.0	150.0	6.8	40.0	6.195	0.039	0.986	
17	7.0	150.1	8.0	38.7	6.188	0.045	0.985	
18	6.9	150.0	6.7	40.0	6.183	0.039	0.984	
19	6.8	151.5	8.0	40.0	6.170	0.044	0.982	
20	7.0	150.0	6.5	40.0	6.170	0.038	0.982	

Table 5
Different types of adsorbent used for Ni^{2+} removal and their adsorption capacity

Adsorbent type	Adsorption capacity	References
Alkali-modified biochar	0.89 mg g^{-1}	[39]
Clay	19.4 mg g^{-1}	[40]
Tea waste	5.4 mg g^{-1}	
Astragalus plant	1.3 mg g^{-1}	
Chestnut shell	5.6 mg g^{-1}	
Eggshell	72.0 mg g^{-1}	
Agaricus bisporus	54.12 mg g^{-1}	[41]
Amanita caesarea	0.76 mg g^{-1}	[42]
Amanita rubescens (fruiting bodies)	52.1 g kg^{-1} and 293 mg kg^{-1}	[43]
Amanita strobiliformis	3.02 mg kg^{-1}	[44]
Amanita vaginata	2.07 mg kg^{-1}	
Amanita phalloides	7.23 mg kg^{-1}	
Amanita muscaria	2.24 mg kg^{-1}	
Pleurotus ostreatus	0.4 mg g^{-1}	[45]
Agaricus bisporus	7.9 mg g^{-1}	
Rice husk	12.41 mg g^{-1}	[46]
Pistachio hull waste	14 mg g^{-1}	[47]
Non-living *Sargassum hemiphyllum*	42.95 mg g^{-1}	[48]
Kenaf fiber/chitosan	70.55 mg g^{-1}	[49]
Aloe barbadensis Miller waste leaves powder	10 mg g^{-1}	[50]
Lansium domesticum peel	10.1 mg g^{-1}	[51]
Three-dimensional macroporous cellulose-based bioadsorbent	171.8 mg g^{-1}	[52]
Hass avocado (*Persea americana Mill var. Hass*) shell	126.3 mg g^{-1}	[53]
Lemon peel waste	0.626 mmol g^{-1}	[54]
Tannin-based dithiocarbamate	112.49 mg g^{-1}	[55]
Padina sanctae-crucis	78.74 mg g^{-1}	[56]
Custard apple seeds and *Aspergillus niger*	10 g L^{-1}	[57]
Jackfruit peel	12.03 mg g^{-1}	[58]
Succinylated hay	57.77 mg g^{-1}	[59]
Amino-functionalized lignin microspheres	49.42 mg g^{-1}	[60]
Date seeds powder	41.0 mg g^{-1}	[61]

advantages such as high adsorption capacity and reuse potential, it is eco-friendly and superior to some other adsorbents for the removal of Ni^{2+} ions from wastewater.

3.1.5. Biocomposite material reuse studies

For understanding whether the adsorption–desorption process is damaging to used material as adsorbent and for testing adsorbent reusability potential several repeat experiments were performed. Because reuse process especially due to the chemicals used in this step can be damaged the biological structure of adsorbent material. In addition, desorption studies help to understand and clarify adsorption process nature. Also, after the use in any adsorption system, recovering the adsorbate and reuse is a desirable situation since it reduces the cost and proves to be a qualified adsorbent.

Experimental studies clearly showed that after the adsorption process, Ni^{2+} ions were removed from the aqueous solution at a rate of about 99%. Moreover, it was observed that the solvents used for desorption separated 99% of the Ni^{2+} ions adsorbed from the surface of the biocomposite material. Afterward process of desorption, based on previous optimum conditions, Ni^{2+} ions were again adsorbed on the biocomposite material surface. The Ni^{2+} ions application studies to the biocomposite material were repeated at least 8 times. Results revealed that percentages of desorption efficiency were calculated to be higher than 98% (Fig. 8). The reuse and repeated use potential of biocomposite material was found to be good. As highlighted, the biocomposite material's good regenerates and reuse ability has considerably an advantage in its application for Ni^{2+} ions removal from IW.

4. Conclusion

In this study, the biocomposite material obtained by using *A. vaginata* mushroom and XAD-4 was used to determine the removal capacity of Ni^{2+} ions from IW and the achieved results indicated that biocomposite material has

a high adsorption capacity. Due to the high adsorption capacity of the produced biocomposite material, it can also be used for the removal of other elements. It is also an advantage that the material used in adsorbent production is a natural material. When the RSM graphs and results were examined, it was determined that pH, initial concentration, and the amount of biocomposite material were the most effective parameters on the adsorption capacity of the adsorbent, but the solution flow rate was not effective. To reach a global optimal solution for maximizing the removal of Ni^{2+} ions from wastewater using biocomposite material a CCD optimization procedure was performed. To find out a suitable model leading to optimum outcome conditions (pH of solution: 6.9, biocomposite material amount: 150.1 mg, solution flow rate: 7.8 mL min^{-1}, and initial concentration of Ni^{2+} ions: 39.7 mg L^{-1}) a CCD method was identified to yield a maximum Ni^{2+} ions removal of 99%. Obtained R^2 (0.9887) and R^2_{adj} (0.9782) values from the ANOVA were satisfactory. Moreover, it can be said that 98.87% of the model-predicted values matched the experimental adsorbed Ni^{2+} ions values on biocomposite material. Used biocomposite material adsorption capacity for Ni^{2+} ions was found as 6.28 mg g^{-1}. It has also been found that the biocomposite material can be used at least eight times for Ni^{2+} ions removal, which indicates good reusability potential.

Conflict of interest statement

The authors declare that they have no known competing financial interests or personal relationships that could have appeared to influence the work reported in this paper.

Research and publication ethics statement

The author declares that this study complies with research and publication ethics.

Data availability statement

Data sets used and/or analyzed during this study can be obtained from appropriate authors upon reasonable request.

References

[1] B. Qin, H. Luo, G. Liu, R. Zhang, S. Chen, Y. Hou, Y. Luo, Nickel ion removal from wastewater using the microbial electrolysis cell, Bioresour. Technol., 121 (2012) 458–461.
[2] A. Bhatnagar, A.K. Minocha, Biosorption optimization of nickel removal from water using *Punica granatum* peel waste, Colloids Surf., B, 76 (2010) 544–548.
[3] M.G.A. Vieira, A.F. Almeida Neto, M.L. Gimenes, M.G.C. da Silva, Sorption kinetics and equilibrium for the removal of nickel ions from aqueous phase on calcined Bofe bentonite clay, J. Hazard. Mater., 177 (2010) 362–371.
[4] N. Boujelben, J. Bouzid, Z. Elouear, Adsorption of nickel and copper onto natural iron oxide-coated sand from aqueous solutions: study in single and binary systems, J. Hazard. Mater., 163 (2009) 376–382.
[5] E. Katsou, S. Malamis, K.J. Haralambous, M. Loizidou, Use of ultrafiltration membranes and aluminosilicate minerals for nickel removal from industrial wastewater, J. Membr. Sci., 360 (2010) 234–249.
[6] E. Denkhaus, K. Salnikow, Nickel essentiality, toxicity, and carcinogenicity, Crit. Rev. Oncol. Hematol., 42 (2002) 35–56.
[7] M.A.K.M. Hanafiah, H. Zakaria, W.S.W. Ngah, Base treated cogon grass (*Imperata cylindrica*) as an adsorbent for the removal of Ni(II): kinetic, isothermal and fixed-bed column studies, CLEAN – Soil, Air, Water, 38 (2010) 248–256.
[8] USEPA, Guidelines For Water Reuse, United States Environmental Protection Agency, 2004.
[9] M. El-Sadaawy, O. Abdelwahab, Adsorptive removal of nickel from aqueous solutions by activated carbons from doum seed (*Hyphaenethebaica*) coat, Alexandria Eng. J., 53 (2014) 399–408.
[10] H. Kalavathy, B. Karthik, L.R. Miranda, Removal and recovery of Ni and Zn from aqueous solution using activated carbon from *Hevea brasiliensis*: batch and column studies, Colloids Surf., B, 78 (2010) 291–302.
[11] R. Sharma, B. Singh, Removal of Ni(II) ions from aqueous solutions using modified rice straw in a fixed-bed column, Bioresour. Technol., 146 (2013) 519–524.
[12] J. Febrianto, A.N. Kosasih, J. Sunarso, Y.-H. Ju, N. Indraswati, S. Ismadji, Equilibrium and kinetic studies in adsorption of heavy metals using biosorbent: a summary of recent studies, J. Hazard. Mater., 162 (2009) 616–645.
[13] E. Gutiérrez-Segura, A. Colín-Cruz, C. Fall, M. Solache-Ríos, P. Balderas-Hernández, Comparison of Cd–Pb adsorption on commercial activated carbon and carbonaceous material from pyrolysed sewage sludge in column system, Environ. Technol., 30 (2009) 455–461.
[14] S.M. Nomanbhay, K. Palanisamy, Removal of heavy metal from industrial wastewater using chitosan coated oil palm shell charcoal, Electron. J. Biotechnol., 8 (2005) 43–53.
[15] E. Malkoc, Y. Nuhoglu, Removal of Ni(II) ions from aqueous solutions using waste of tea factory: adsorption on a fixed-bed column, J. Hazard. Mater., 135 (2006) 328–336.
[16] B. Fonseca, A. Teixeira, H. Figueiredo, T. Tavares, Modelling of the Cr(VI) transport in typical soils of the North of Portugal, J. Hazard. Mater., 167 (2009) 756–762.
[17] N. Miralles, C. Valderrama, I. Casas, M. Martínez, A. Florido, Cadmium and lead removal from aqueous solution by grape stalk wastes: modeling of a fixed-bed column, J. Chem. Eng. Data, 55 (2010) 3548–3554.
[18] V.A. Lemos, P.X. Baliza, Amberlite XAD-2 functionalized with 2-aminothiophenol as a new sorbent for on-line preconcentration of cadmium and copper, Talanta, 67 (2005) 564–570.
[19] M. Dogru, R. Gul-Guven, S. Erdogan, The use of *Bacillus subtilis* immobilized on Amberlite XAD-4 as a new biosorbent in trace metal determination, J. Hazard. Mater., 149 (2007) 166–173.
[20] E.J. dos Santos, A.B. Herrmann, A.S. Ribeiro, A.J. Curtius, Determination of Cd in biological samples by flame AAS following on-line preconcentration by complexation with *O,O*-diethyldithiophosphate and solid phase extraction with Amberlite XAD-4, Talanta, 65 (2005) 593–597.
[21] S. Baytak, A. Rehber Türker, The use of *Agrobacterium tumefaciens* immobilized on Amberlite XAD-4 as a new biosorbent for the column preconcentration of iron(III), cobalt(II), manganese(II) and chromium(III), Talanta, 65 (2005) 938–945.
[22] S. Özdemir, R. Gul-Guven, E. Kilinc, M. Dogru, S. Erdogan, Preconcentration of cadmium and nickel using the bioadsorbent *Geobacillus thermoleovorans* subsp. *stromboliensis* immobilized on Amberlite XAD-4, Microchim. Acta, 169 (2010) 79–85.
[23] K.H. Chu, Improved fixed-bed models for metal biosorption, Chem. Eng. J., 97 (2004) 233–239.
[24] B.C. Pan, F.W. Meng, X.Q. Chen, B.J. Pan, X.T. Li, W.M. Zhang, X. Zhang, J.L. Chen, Q.X. Zhang, Y. Sun, Application of an effective method in predicting breakthrough curves of fixed-bed adsorption onto resin adsorbent, J. Hazard. Mater., 124 (2005) 74–80.
[25] B. Volesky, Detoxification of metal-bearing effluents: biosorption for the next century, Hydrometallurgy, 59 (2001) 203–216.
[26] J. Qu, T. Song, J. Liang, X. Bai, Y. Li, Y. Wei, S. Huang, L. Dong, Y. Jin, Adsorption of lead(II) from aqueous solution by modified *Auricularia* matrix waste: a fixed-bed column study, Ecotoxicol. Environ. Saf., 169 (2019) 722–729.
[27] M. Ince, O. Kaplan Ince, Application of response surface methodological approach to optimize removal of Cr ions from industrial wastewater, At. Spectrosc., 40 (2019) 91–97.

[28] O. Kaplan Ince, M. Ince, A. Onal, Response surface modeling for Pb(II) removal from alcoholic beverages using natural clay: process optimization with Box–Behnken experimental design and determination by electrothermal AAS, At. Spectrosc., 39 (2018) 242–250.

[29] M.N.V. Ravi Kumar, A review of chitin and chitosan applications, React. Funct. Polym., 46 (2000) 1–27.

[30] Ş. Alpat, S. Kilinç Alpat, B. Hilal Çadirci, Ö. Özbayrak, İ. Yasa, Effects of biosorption parameter: kinetics, isotherm and thermodynamics for Ni(II) biosorption from aqueous solution by *Circinella* sp., Electron. J. Biotechnol., 13 (2010) 1–19.

[31] T. Eticha, A. Hymete, Health risk assessment of heavy metals in locally produced beer to the population in Ethiopia, J. Bioanal. Biomed., 6 (2014) 65–68.

[32] S. Zou, H. Wang, X. Wang, S. Zhou, X. Li, Y. Feng, Application of experimental design techniques in the optimization of the ultrasonic pretreatment time and enhancement of methane production in anaerobic co-digestion, Appl. Energy, 179 (2016) 191–202.

[33] S. Perincek, K. Duran, Optimization of enzymatic & ultrasonic bio-scouring of linen fabrics by aid of Box–Behnken Experimental Design, J. Cleaner Prod., 135 (2016) 1179–1188.

[34] H. Bakraouy, S. Souabi, K. Digua, O. Dkhissi, M. Sabar, M. Fadil, Optimization of the treatment of an anaerobic pretreated landfill leachate by a coagulation–flocculation process using experimental design methodology, Process Saf. Environ. Prot., 109 (2017) 621–630.

[35] J.N. Sahu, J. Acharya, B.C. Meikap, Response surface modeling and optimization of chromium(VI) removal from aqueous solution using Tamarind wood activated carbon in batch process, J. Hazard. Mater., 172 (2009) 818–825.

[36] A. Asfaram, M. Ghaedi, S. Hajati, M. Rezaeinejad, A. Goudarzi, M.K. Purkait, Rapid removal of Auramine-O and Methylene blue by ZnS:Cu nanoparticles loaded on activated carbon: a response surface methodology approach, J. Taiwan Inst. Chem. Eng., 53 (2015) 80–91.

[37] E.A. Dil, M. Ghaedi, A. Ghaedi, A. Asfaram, M. Jamshidi, M.K. Purkait, Application of artificial neural network and response surface methodology for the removal of crystal violet by zinc oxide nanorods loaded on activate carbon: kinetics and equilibrium study, J. Taiwan Inst. Chem. Eng., 59 (2016) 210–220.

[38] M. Ince, O. Kaplan Ince, Box–Behnken design approach for optimizing removal of copper from wastewater using a novel and green adsorbent, At. Spectrosc., 38 (2017) 200–207.

[39] Z. Ding, X. Hu, Y. Wan, S. Wang, B. Gao, Removal of lead, copper, cadmium, zinc, and nickel from aqueous solutions by alkali-modified biochar: batch and column tests, J. Ind. Eng. Chem., 33 (2016) 239–245.

[40] M. Ince, Comparision of low-cost and eco-friendly adsorbent for adsorption of Ni(II), At. Spectrosc., 35 (2014) 223–233.

[41] S.C. Sithole, L.L. Mugivhisa, S.O. Amoo, J.O. Olowoyo, Pattern and concentrations of trace metals in mushrooms harvested from trace metal-polluted soils in Pretoria, South Africa, S. Afr. J. Bot., 108 (2017) 315–320.

[42] P.K. Ouzouni, D. Petridis, W.-D. Koller, K.A. Riganakos, Nutritional value and metal content of wild edible mushrooms collected from West Macedonia and Epirus, Greece, Food Chem., 115 (2009) 1575–1580.

[43] M. Rudawska, T. Leski, Macro- and microelement contents in fruiting bodies of wild mushrooms from the Notecka forest in west-central Poland, Food Chem., 92 (2005) 499–506.

[44] J. Vetter, Mineral composition of basidiomes of *Amanita* species, Mycol. Res., 109 (2005) 746–750.

[45] Ö. Isildak, I. Turkekul, M. Elmastas, M. Tuzen, Analysis of heavy metals in some wild-grown edible mushrooms from the middle black sea region, Turkey, Food Chem., 86 (2004) 547–552.

[46] H. Basu, S. Saha, I.A. Mahadevan, M.V. Pimple, R.K. Singhal, Humic acid coated cellulose derived from rice husk: a novel biosorbent for the removal of Ni and Cr, J. Water Process Eng., 32 (2019) 100892, doi: 10.1016/j.jwpe.2019.100892.

[47] M. Zamani Beidokhti, S. Taghi (Omid) Naeeni, M.S. AbdiGhahroudi, Biosorption of nickel(II) from aqueous solutions onto pistachio hull waste as a low-cost biosorbent, Civ. Eng. J., 5 (2019) 447–457.

[48] X. Fan, J. Xia, J. Long, The potential of nonliving *Sargassum hemiphyllum* as a biosorbent for nickel(II) removal—isotherm, kinetics, and thermodynamics analysis, Environ. Prog. Sustainable Energy, 38 (2019) S250–S259.

[49] J. Annie Kamala Florence, T. Gomathi, N. Thenmozhi, P.N. Sudha, Adsorption study: removal of nickel ions using Kenaf fiber/chitosan biosorbent, J. Chem. Pharm. Res., 7 (2015) 410–422.

[50] S. Gupta, A. Kumar, Removal of nickel(II) from aqueous solution by biosorption on *A. barbadensis Miller* waste leaves powder, Appl. Water Sci., 9 (2019) 96, doi: 10.1007/s13201-019-0973-1.

[51] Y.F. Lam, L.Y. Lee, S.J. Chua, S.S. Lim, S. Gan, Insights into the equilibrium, kinetic and thermodynamics of nickel removal by environmental friendly *Lansium domesticum* peel biosorbent, Ecotoxicol. Environ. Saf., 127 (2016) 61–70.

[52] L. Liu, J.P. Xie, Y.J. Li, Q. Zhang, J.M. Yao, Three-dimensional macroporous cellulose-based bioadsorbents for efficient removal of nickel ions from aqueous solution, Cellulose, 23 (2016) 723–736.

[53] D.E. Vazquez-Palma, A.R. Netzahuatl-Munoz, G. Pineda-Camacho, E. Cristiani-Urbina, Biosorptive removal of nickel(II) ions from aqueous solutions by hass avocado (*Persea Americana mill. Var. Hass*) shell as an effective and low-cost biosorbent, Fresenius Environ. Bull., 26 (2017) 3501–3513.

[54] M. Villen-Guzman, M.M. Cerrillo-Gonzalez, J.M. Paz-Garcia, J.M. Rodriguez-Maroto, B. Arhoun, Valorization of lemon peel waste as biosorbent for the simultaneous removal of nickel and cadmium from industrial effluents, Environ. Technol. Innovation, 21 (2021) 101380, doi: 10.1016/j.eti.2021.101380.

[55] C. Zhao, H. Zheng, Y. Sun, B. Liu, Y. Zhou, Y. Liu, X. Zheng, Fabrication of tannin-based dithiocarbamate biosorbent and its application for Ni(II) ion removal, Water Air Soil Pollut., 228 (2017) 409, doi: 10.1007/s11270-017-3593-0.

[56] R. Foroutan, H. Esmaeili, A.M. Sanati, M. Ahmadi, B. Ramavandi, Adsorptive removal of Pb(II), Ni(II), and Cd(II) from aqueous media and leather wastewater using *Padina sanctae-crucis* biomass, Desal. Water Treat., 135 (2018) 236–246.

[57] A. Saravanan, P. Senthil Kumar, B. Preetha, Optimization of process parameters for the removal of chromium(VI) and nickel(II) from aqueous solutions by mixed biosorbents (custard apple seeds and *Aspergillus niger*) using response surface methodology, Desal. Water Treat., 57 (2016) 14530–14543.

[58] S.H. Ranasinghe, A.N. Navaratne, N. Priyantha, Enhancement of adsorption characteristics of Cr(III) and Ni(II) by surface modification of jackfruit peel biosorbent, J. Environ. Chem. Eng., 6 (2018) 5670–5682.

[59] P. Lin, J. Wu, J. Ahn, J. Lee, Adsorption characteristics of Cd(II) and Ni(II) from aqueous solution using succinylated hay, Int. J. Miner. Metall. Mater., 26 (2019) 1239–1246.

[60] A.L. Popovic, J.D. Rusmirovic, Z. Velickovic, Z. Radovanovic, M. Ristic, V.P. Pavlovic, A.D. Marinkovic, Novel amino-functionalized lignin microspheres: high performance biosorbent with enhanced capacity for heavy metal ion removal, Int. J. Biol. Macromol., 156 (2020) 1160–1173.

[61] A. Elkhaleefa, I.H. Ali, E.I. Brima, A.B. Elhag, B. Karama, Efficient removal of Ni(II) from aqueous solution by date seeds powder biosorbent: adsorption kinetics, isotherm and thermodynamics, Processes, 8 (2020) 1001, doi: 10.3390/pr8081001.